Proceedings World Geothermal Congress 2020+1
Reykjavik, Iceland, April - October 2021

He-CO$_2$-N$_2$ Isotope and Relative Abundance Characterization of Geothermal Fluids from the Ethiopian Rift

S.A. Halldórsson[1*], P. Scarsi[2], T. Abebe[2], T. Evans[3], J.T. Kulongoski[3,4], P.R. Castillo[3], P.H. Barry[5], D.R. Hilton[3†]

1: NordVulk, Institute of Earth Sciences, University of Iceland, Reykjavík, Iceland

2: Institute of Geosciences and Earth Resources, National Research Council of Italy, Pisa, Italy
3: Scripps Institution of Oceanography, UCSD, La Jolla, CA, USA

4: California Water Science Center, USGS, San Diego, CA, USA

5: Woods Hole Oceanographic Institution, Woods Hole, MA, USA

(†deceased)

*Contact: saemiah@hi.is

Keywords: East African Rift, Ethiopia, geothermal fluids, helium isotopes, carbon isotopes, nitrogen isotopes

ABSTRACT

We report He-CO$_2$-N$_2$ isotopic and relative abundances in free gases and dissolved gas phase of geothermal fluids from the Ethiopian Rift. Fluid samples were collected from ~30 geothermal localities from three key regions throughout rifted and non-rifted areas of Ethiopia. The majority of samples, including off-rift samples, indicate a strong contribution of mantle-derived He-C-N to the fluid samples. Helium (^{3}He/^{4}He) and δ^{15}N-(N$_2$) isotope anomalies are highest (> 15.9R$_A$ and > +5.0‰, respectively) at a single locality in south Afar (Sodere), but the maximum δ^{13}C-(CO$_2$) (-0.78‰) is found east of Lake Shalla in the Lake District of the Main Ethiopian Rift. High ^{3}He/^{4}He values, consistent with mantle plume contributions, are also evident in fluids from the Lake District, where fluids from the Lake Shalla site extend up to 15.5R$_A$. CO$_2$/^{3}He values span over four orders of magnitude while δ^{13}C-(CO$_2$) values cluster mostly between mantle-like values of -4 and -7‰; only samples east of Lake Shalla display more positive values. Atmospheric-derived nitrogen has likely influenced a number of measured δ^{15}N-(N$_2$) values but following a correction for atmospheric-contamination, the majority of samples reveal positive values (up to 6.5‰) which appear to be coupled to high ^{3}He/^{4}He values. In regions affected by upwelling mantle plumes, such high values have been interpreted to reflect deep mantle inputs of recycled nitrogen.

1. INTRODUCTION

The East Africa Rift System (EARS), a region in east Africa where the Nubian and Somalian plates are diverging, represents a region of considerable geological interest as it integrates a variety of mantle and crustal processes leading to the formation of a nascent ocean basin. In the northern part of the EARS, the rift extends from the Afar Depression in northern Ethiopia to the southern tip of the Ethiopian Rift. This region remains one of the more studied segments of the EARS but complete geochemical characterization of volatile elements are still incomplete, despite their potential utility in identifying mantle contributions to present-day volcanism, differentiating inputs from various mantle endmembers, and recording and quantifying the effects of additions of crustal volatiles.

Although considerable work has been carried out to date on the He isotope systematics of the Ethiopian rift and Afar (see for example Marty et al. 1996; Scarsi and Craig, 1996, Rooney et al. 2012; Halldórsson et al., 2014) detailed studies of geothermal fluids from which other deeply-derived volatile elements can be extracted, are still lacking. Geothermal fluids are particularly important for establishing the spatial distribution of volatile characteristics in regions affected by upwelling plumes as mafic crystal-bearing lavas are often restricted to geographically small areas (e.g., Harðardóttir et al., 2018).

Craig and Lupton (1977) reported the first and most comprehensive survey of volatiles along this part of the EARS. The focus of that study was the characterization of stable isotope variations (D/H and δ^{18}O) of surface waters, groundwaters, geothermal fluids and steam in the Lakes District of Ethiopia. For this work, approximately 36 samples (20 waters and 16 gases – many from the same locality) were analyzed for He isotopes. The remarkable finding was that the air-corrected ^{3}He/^{4}He ratios varied between 1 and 14.2 R$_A$ – with the highest values (> MORB values) found at 4 sites only. Sampling localities were mainly situated within the Ethiopian Rift to the south of Addis Ababa. Their data generally displayed lower ^{3}He/^{4}He values (< 8 – 10 R$_A$), but only the most southerly site (Nech Sar) had considerable radiogenic helium inputs (2.3 R$_A$). Additionally, Craig and Lupton (1977) reported values between 8 and 10 R$_A$ for two sites in the Afar region (Fig. 3). They ascribed the occurrence of such high ^{3}He/^{4}He ratios in the geothermal fluids of Ethiopia to an association with recent basalts in the vicinity of the geothermal sites.

Later igneous rock-focused studies (e.g., Marty et al., 1996; Scarsi and Craig, 1996) reported ^{3}He/^{4}He values as high as 17 R$_A$ at 8°N in the Ethiopian Rift and 14.2 R$_A$ in the central Tat'Ali sector of the Afar Depression. Significantly, these helium isotope values showed good agreement with fluid ^{3}He/^{4}He ratios measured previously (Craig and Lupton, 1977), and were ascribed to the influence of a deep mantle plume as the force driving rifting processes in the EARS. These unique volatile isotopic characteristics - the high ^{3}He/^{4}He provinces of the Ethiopian Rift in the Lake District and in the Afar Depression - can be defined and exploited to map the spatial extent of the Afar/Ethiopian plume. However, subsequent studies of geothermal fluids rely upon relatively few samples from restricted areas, such as in recent studies in Dallol (Darrah et al., 2013) and North of Lake Abaya (Minnissale, et al., 2017), limiting characterization of the larger extent of the plume.

By integrating helium isotopes with other volatile tracers, our aim is to assess and characterize mantle contributions relative to shallow crustal/lithospheric gas signatures, provide an overview of the distribution of mantle volatiles and detail the processes of mantle volatile transport in this dynamic part of the East African Rift System. Complementary datasets will allow us to both characterize the waters and evaluate the degree of secondary modifications, such as via water-rock interaction In addition, we will assess the significance of correlations – or lack thereof – between these volatile isotopes to distinguish between regional mantle volatile sources and secondary processes which act to modify source-derived signatures.

2. SAMPLE COLLECTION AND METHODS

Fluids samples were collected from ~30 geothermal localities from three key regions throughout rifted and non-rifted areas of Ethiopia. Rifted areas include (i) The Lake District along the Ethiopian Rift – as far south as the Hamasa River (Lake Abaya), and (ii) Southern Afar from Tullu Moye in the south to Gewane in the north. Two off-rift localities from west of the capital, Addis Ababa, Ambo and the Wenchi Caldera, were also sampled. Fluid samples were collected from cool water springs, bubbling hot springs, fumarole and geothermal wells (Figure 1). Select samples have been analyzed for total gas chemistry, including hydrocarbons and δ^{13}C-(CH_4). Additionally, we complement this dataset with chemical analysis of major ion chemistry in the water phase samples as well and water isotopes (δD and δ^{18}O) for the majority of the fluids analyzed.

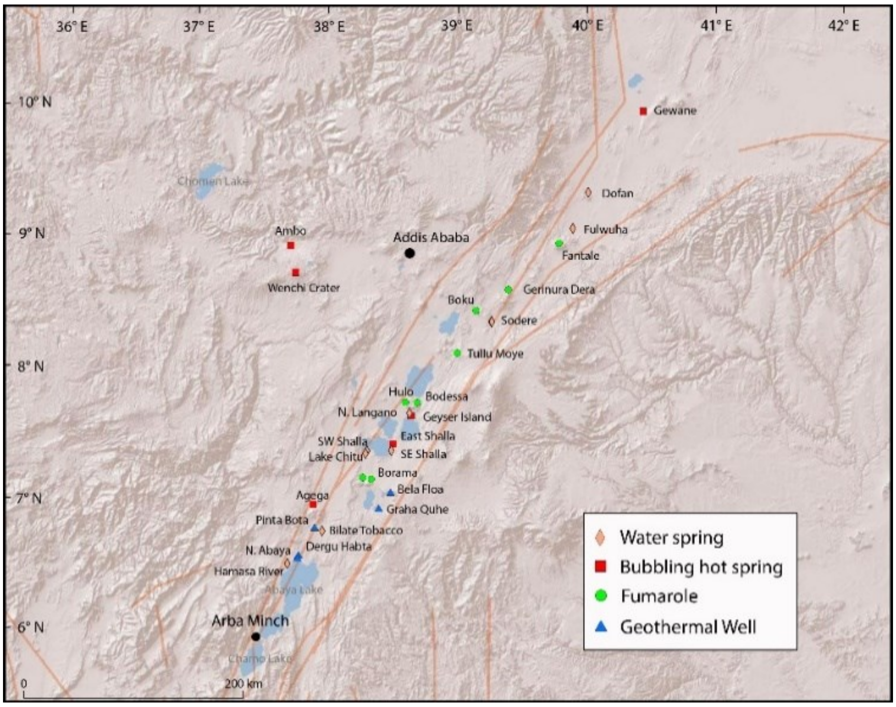

Figure 1: Sample locations in Ethiopia and sample types.

Sampling protocols and analytical procedures for He-CO_2-N_2 isotopic analyses adopted follow closely those described in Halldórsson et al. (2013) and were all performed at the Scripps Institution of Oceanography. Soluble ions were analyzed at the USGS San Diego Water Quality Laboratory by using ion chromatography (U.S. Environmental Protection Agency, 1993). Stable isotopes of water (δD and δ^{18}O) were analyzed using a Picarro L2130-i cavity ring-down laser spectroscopy (CRDS) instrument with auto sampler, calibrated with Vienna vSMOW2, GISP, and SLAP2 reference standards. The scale bar in the lower left corner is 200 km.

3. RESULTS

3.1 Water isotopes and fluids types

Relationships between δD and δ^{18}O values for Ethiopian geothermal fluids are plotted in Figure 2 along with an average of Local Meteoric Water Lines for the region (gray shaded area: LMWL), defined by precipitation collected from IAEA specific sites of basins close to sampling sites, and the GMWL (Global Meteoric Water Line). Our water isotope data are in good agreement with previous data collected for Ethiopian thermal fluids. Although LMWL reveals different slopes, the majority of our fluid samples appear to be not strongly shifted from the GMWL because of evaporation and condensation, water-rock interaction, and mixing with non-meteoric waters.

Major ion chemistry of the water phase samples enables classifications of water types. A ternary plot based on the relative proportions of chloride, sulphate and bicarbonate ions was used to classify geothermal waters (Fig. 2). With the exception of samples from East Shalla, Gewane, Geyser Island and, to a limited extent samples from Dofan, most samples display relatively low chloride content, which is usually regarded as a proxy of waters fed directly from deep reservoirs with minimal mixing or conductive cooling. The majority of water samples can be classified as "steam-heated waters or "steam condensates", as evident by them being particularly rich in bicarbonate. pH values ranged between 6 and 9 and only one sample from west of the Corbetti Caldera revealed lower pH (to 5).

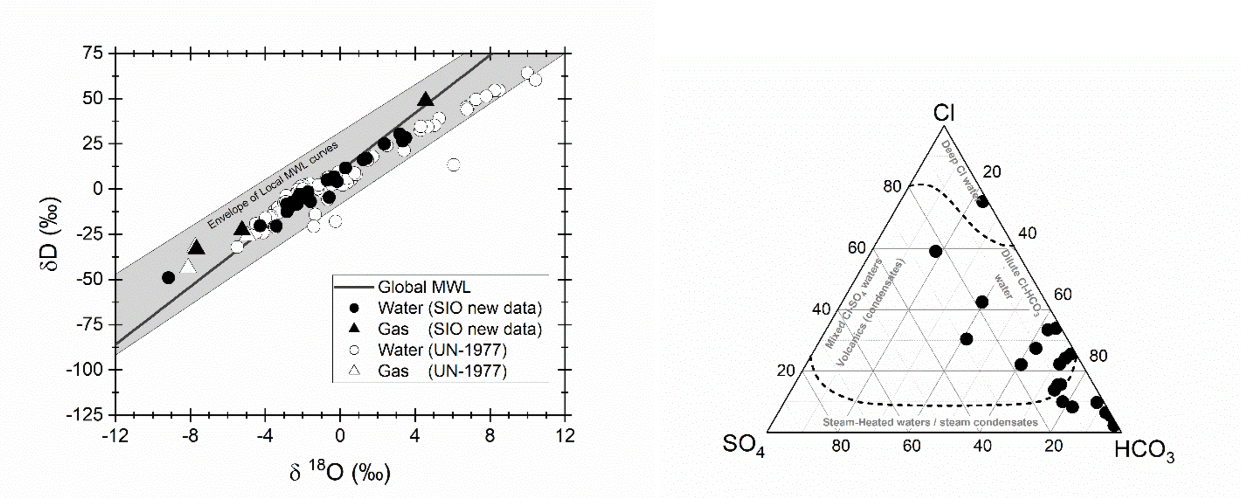

Figure 2: Water isotopes and fluid types: (left) The relationship between δD and $\delta^{18}O$ values for Ethiopian thermal fluids. (right) Ternary plot based on the relative proportions of chloride, sulphate and bicarbonate ions. Additional data from Craig and Lupton (1977).

3.2 Major gas chemistry

13 samples from equally many localities were analyzed for their major gas compositions and for samples not overwhelmed with air-contamination – observed at six low flux localities – CO_2 is the dominant dry-gas species with 6 out of 13 gases having over ~80% (dry gas) CO_2. In those samples, nitrogen is the most abundant dry-gas species, ranging from ~0.6% to ~17%. When detected, hydrogen was always lower than 0.046%.

3.3 Helium isotopes

54 samples from 29 localities were analyzed, 26 of which were analyzed in duplicates. In Figure 3, we plot measured He isotopes (R_M/R_A) (including duplicates) versus solubility-corrected, air-normalized He/Ne ratio (X) to assess the integrity of the He isotope results. Measured $^3He/^4He$ ratios (reported as R_M/R_A where R_M = measured $^3He/^4He$ of sample and R_A = $^3He/^4He$ of air; $1.4\text{x}10^{-6}$) have been corrected (to R_C/R_A) for the presence of atmospheric components using the air-normalized He/Ne ratio multiplied by the ratio of the Bunsen coefficients, assuming an air-equilibration temperature of 15°C (= X value). For the most part, the correction results in minor changes to the measured $^3He/^4He$ (R_M/R_A) ratio but we note that the X values for some of these samples are exceptionally low (<5) and thus these samples have likely experienced significant atmospheric contamination.

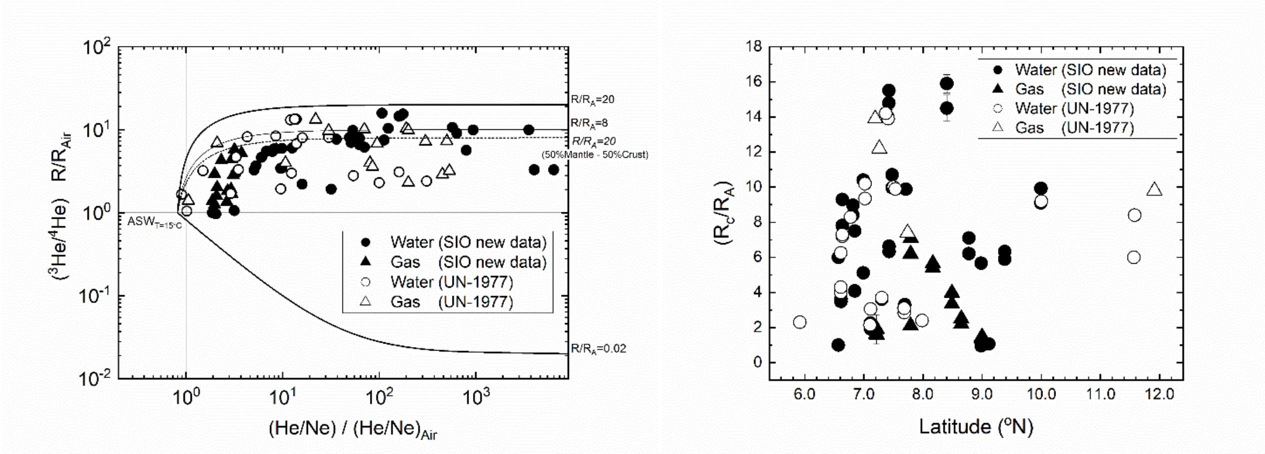

Figure 3: Helium isotopes: (left) measured He isotopes vs. X-value (right) Air-corrected He isotopes correct vs. latitude. Additional data from Craig and Lupton (1977).

In general, our new He isotope data are in good agreement with previous He isotope data collected for Ethiopian thermal fluids (Fig. 3 –right). As was demonstrated by Scarsi and Craig (1996), there is good correspondence between He isotope data produced utilizing geothermal fluids and lavas. In this case, both basalts and geothermal fluids from the Ethiopian Rift reveal the presence of a high-$^3He/^4He$ domain with values as high as ~16R_A in a broad region which extends from south Afar (~9°N) to the Lake District of the Ethiopian Rift (~7°N).

3.4 Carbon and nitrogen isotopes

The $\delta^{13}C$-(CO_2) values of all gas and water phase samples (including duplicates) are shown in Figure 4 (plotted vs. $CO_2/^3He$). The $\delta^{13}C$-(CO_2) values range from -0.77‰ to -10.77‰. Notably, $\delta^{13}C$-(CO_2) values cluster between -4 and -7‰ and only the values east of Lake Shalla display more positive values. Majority of the $\delta^{13}C$-(CO_2) values are therefore very similar to values which are generally thought to be representative for the depleted MORB mantle (e.g., Cartigny et al., 2014). In contrast, the molar ratio of $CO_2/^3He$ varies by over 4 orders of magnitude, from 0.0025 × 10^9 to 542 × 10^{12}.

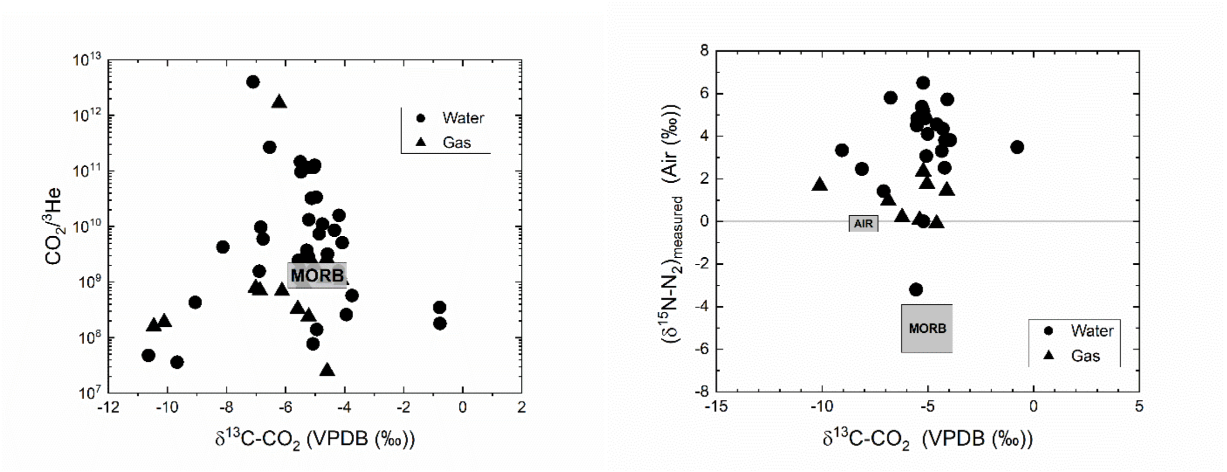

Figure 4: Stable isotopes and $CO_2/^3He$. (left) $CO_2/^3He$ vs. $\delta^{13}C$-(CO_2 (right) $\delta^{13}C$-(CO_2) vs. $\delta^{15}N$-(N_2). The MORB-box indicates values which are generally thought to be representative for the depleted MORB mantle (see text for details).

In Figure 4 (right), we plot measured $\delta^{15}N$-(N_2) vs. $\delta^{13}C$-(CO_2). Measured $\delta^{15}N$ values range from -3.3 to +6.5‰ with the most positive $\delta^{15}N$ values for our dataset being a sample from Sodere but the most negative value a gas samples from Graha Quhe (see Fig. 1). We note that only four fluid samples display $\delta^{15}N$-(N_2) which overlap with air and the majority of samples reveal positive values. It is thus noteworthy that while $\delta^{13}C$-(CO_2) values are remarkably constant and mantle-like, $\delta^{15}N$-(N_2) values are both non-atmospheric and non-mantle-like with $\delta^{15}N$ values more positive than air, prevailing the dataset. In this regard, we note that Darrah et al. (2013) also reported high $\delta^{15}N$-(N_2) values in samples from the Dallol region in Afar (ranged between +3.5 to 4.0‰)

3.5 Hydrocarbons and isotopes

Methane is highly variable but the majority of samples contain less than 1% methane. Three samples (Lake Shalla, Geyser Island and Gewane) display CH_4 concentrations notably higher than all other sample. Of these, the highest CH_4 contents (3.3%) were found in a sample containing ~49% CO_2 east of Lake Shalla.

We analyzed $\delta^{13}C$-(CH_4) in seven of these samples and these range from -46.5‰ to -6.5‰. A sample from east of Lake Shalla which also displays the highest methane/ethane (>1300), has the highest $^3He/^4He$ of all samples analyzed for $\delta^{13}C$-(CH_4) (~10R_A), but the lowest measured $\delta^{13}C$-(CH_4) value (-46.5‰).

4. DISCUSSION

4.1 Identification of modified He, CO_2, N_2 characteristics

A ternary plot (Figure 5-left) of He-C relationships (based on Giggenbach et al., 1993) allows us to assess sample integrity and identify fluid samples which are modified by air contamination, shallow-level crustal contamination and/or elemental fractionation within the hydrothermal systems. A number of water phase samples, as well as one gas phase sample, are characterized by very high $CO_2/^3He$ ratios (up to 542 × 10^{12}) consistent with phase separation, fractionating CO_2 from ^3He and resulting in such high $CO_2/^3He$. This observation is further supported by a strong negative correlation between $CO_2/^3He$ and He concentrations in water phase samples (not plotted). In contrast, water and gas phase samples with low $CO_2/^3He$ have likely been affected by precipitation of calcite at depth (e.g., Halldórsson et al., 2013). The loss of CO_2 following calcite precipitation will result in lower $CO_2/^3He$ in the residual fluid as would be consistent with our data. Moreover, temperature-controlled precipitation of calcite can also modify $\delta^{13}C$-(CO_2) values. In this case, calcite precipitation has likely affected water and gas phase samples that display lower-than-mantle $CO_2/^3He$ and $\delta^{13}C$-(CO_2) values (Figure 4-left). Finally, we also note that several gas phase samples (triangles) with $^3He/^4He < 3R_A$, are likely contaminated by air (Figure 5-left). These sample also underwent a large air-correction to measured He isotope compositions.

To evaluate if atmospheric nitrogen has influence $\delta^{15}N$-(N_2), we plot measured $\delta^{15}N$-(N_2) vs. X-values [(He/Ne_{sample})(He/Ne_{air})]. We note that samples that display X-values below ~100 tend to correlate with measured $\delta^{15}N$-(N_2) values suggesting variable contamination by atmospheric nitrogen for those samples. Therefore, and following Halldórsson et al. (2013), we corrected measured $\delta^{15}N$-(N_2) for the presence of atmospheric nitrogen using an approach similar to that used for He isotopes. This approach, which uses X-values as a proxy for air contamination, will correct measured $\delta^{15}N$-(N_2) away from air, either towards more positive or more negative values. However, the corrected values for this dataset only differ from measured values by up to 0.6‰ (largest for samples with X-values < 10) suggesting that this approach, while relying on independent proxies for air-contamination, is only partially successful in removing samples affected by atmospheric nitrogen.

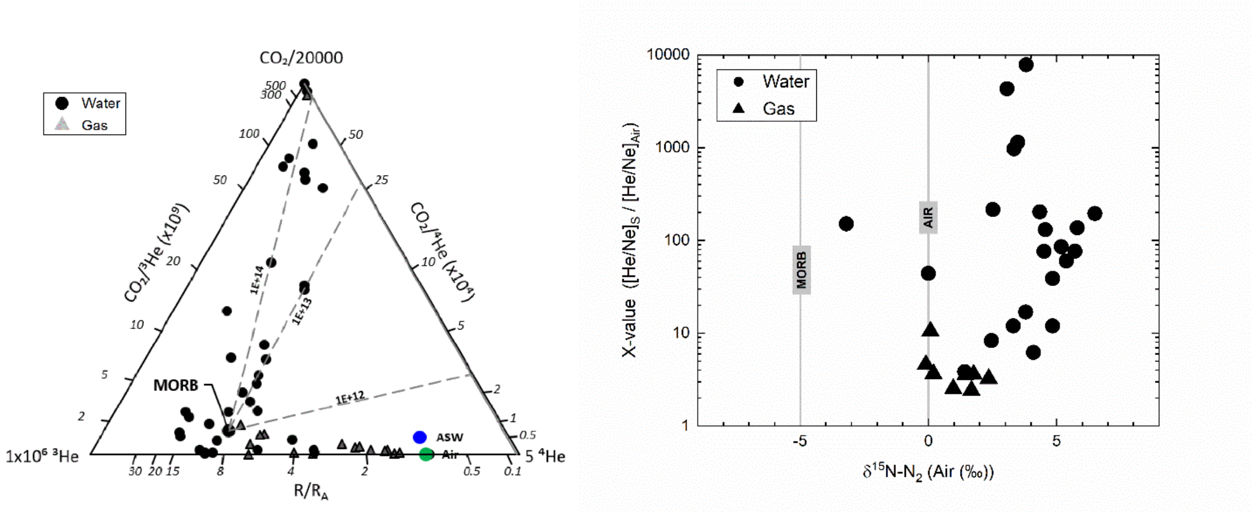

Figure 5: (left) Ternary plot of CO_2, ^3He, and ^4He for Ethiopian geothermal fluids (based on Giggenbach et al., 1993). (right) Measured $\delta^{15}N$-(N_2) vs. air-normalized He/Ne elemental ratios (X-values) multiplied by the ratio of the Bunsen coefficients.

4.2 Integration of helium isotopes with other volatile isotope tracers

Helium isotopes are plotted versus both carbon and nitrogen isotopes in Figure 6. The maximum $\delta^{13}C$-(CO_2) values of -0.78‰ from east of Lake Shalla stand out on this plot, as do the minimum $\delta^{13}C$-(CO_2) values of around -10‰ evident in water and gas samples from Hamasa River and Boku, respectively. As discussed above, such low $\delta^{13}C$-(CO_2) values likely results from precipitation of calcite at depth. For all other samples, we observed no clear relationships between $\delta^{13}C$-(CO_2) values and $^3He/^4He$ and note that most $\delta^{13}C$-(CO_2) values – irrespective of their $^3He/^4He$ values – cluster between -4 and -7‰ and therefore very close to values representative for the depleted MORB mantle (-5 ± 1‰).

Air-corrected $\delta^{15}N$-(N_2) values are plotted vs. air-corrected $^3He/^4He$ in Figure 6 (right). Four fluid samples display $\delta^{15}N$-(N_2) which overlap with air, whereas the majority of air-corrected $\delta^{15}N$-(N_2) values have values greater than +2‰. As evident from Figure 5, samples with X-values above ~100 do not reveal any clear correlation between $\delta^{15}N$-(N_2) and X-values, suggesting that such positive $\delta^{15}N$-(N_2) are indeed a primary feature of Ethiopian geothermal fluids. Moreover, our data clearly show that air-corrected $\delta^{15}N$-(N_2) are dominated by values more positive than air and that some of the highest $\delta^{15}N$-(N_2) values (up to +6.5‰) are found in samples that also display $^3He/^4He$ values. Such positive $\delta^{15}N$-(N_2) are in marked contrast to $\delta^{15}N$-(N_2) values which are generally regarded to be representative of depleted MORB mantle (-5 ± 2‰: Cartigny and Marty, 2013) and more akin to values evident at mantle hotspots.

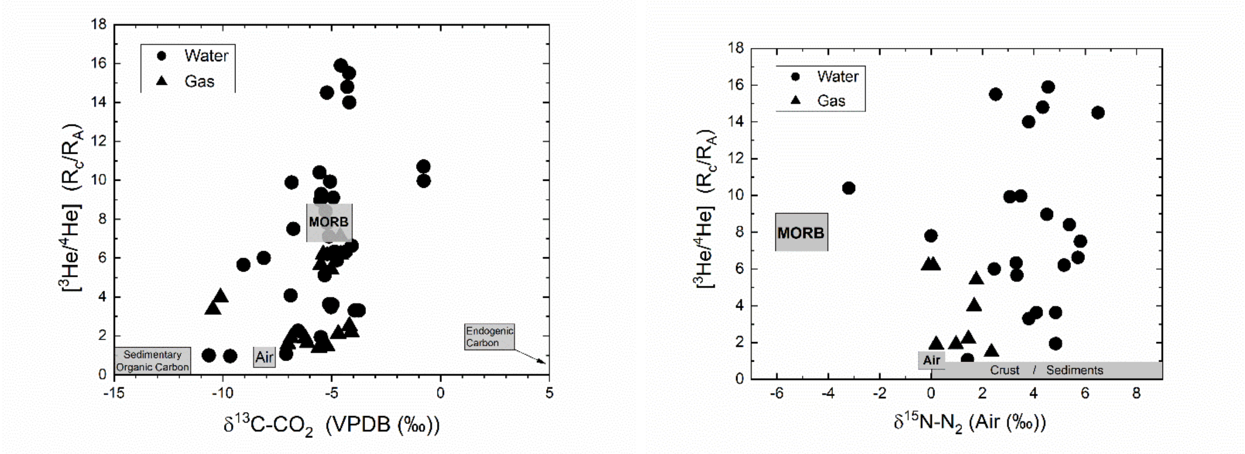

Figure 6: He-C-N isotope relationships in Ethiopian geothermal fluids: (left) He isotopes vs. $\delta^{13}C$-(CO_2) (right) He isotopes vs. $\delta^{15}N$-(N_2) both corrected for air-contamination using X-values.

4.3 Implication for African Superplume volatile supply to rifted areas of Ethiopia

This multi-tracer dataset of geothermal fluids from the Ethiopian Rift has facilitated a detailed characterization of mantle-derived gases associated with volcanism in both rifted and non-rifted areas in Ethiopia. For example, uniform and MORB-like $\delta^{13}C$-(CO_2) evident in Ethiopian geothermal fluids suggest that the high $^3He/^4He$ mantle (i) has $\delta^{13}C$-(CO_2) values identical to those representative for CO_2 extracted from the depleted MORB mantle or (ii) is carbon-depleted and therefore its signature is overwhelmed by mixing with carbon derived from the upper mantle. In contrast, positive $\delta^{15}N$-(N_2) values which appear to be dominantly sampled in Ethiopian geothermal fluids, are akin to mantle hotspot $\delta^{15}N$-(N_2) values. Positive $\delta^{15}N$-(N_2) values at mantle hotspots have been interpreted to reflect sampling of deeply-derived nitrogen which was once at the surface but underwent subduction at divergent plate boundaries but is begin recycled by via upwelling of deep-seated mantle plume (e.g., Barry and Hilton, 2016 and reference therein). This also appears to be the case for nitrogen sample in the volcanic areas of Ethiopia.

In light of recent models that argue for a common plume source underlying the entire EARS (e.g., Castillo et al., 2014; Halldórsson et al., 2014), we argue that the deeply rooted African Superplume, which influences magmatism throughout eastern Africa, supplies volatiles to rifted areas of Ethiopia. Although the sub-continental lithospheric mantle has been argued to play a key role in generating low $^3He/^4He$ along the Western Rift and the southern Kenya rift, the dominance of $^3He/^4He$ values considerably higher than this reservoir (~6 R_A), suggest that this part of the mantle did not greatly affect the C and N characteristic of mantle-derived fluids sampled in Ethiopian geothermal fluids. Rather, and as indicated by both radiogenic isotopes (Castillo et al., 2014) and He-Ne isotope data (Halldórsson et al., 2014) from mantle-derived materials, Ethiopian Rift volatiles are best explained by a simple binary mixing between an upper mantle volatile source and a deep-mantle plume source.

5. CONCLUSIONS

Geothermal fluids from the Ethiopian Rift reveal clear contributions of mantle-derived He-C-N. In agreement with helium isotope data available for basalts, $^3He/^4He$ values as high as ~16R_A are evident in a broad region which extends from south Afar (~9°N) to the Lake District of the Ethiopian Rift (~7°N). Mantle-like $\delta^{13}C$-(CO_2) values are also evident in this broad region further confirming contributions from a mantle volatile source to this region. However, $\delta^{15}N$-(N_2) values are largely more positive than air, reaching values as high as +6.5‰. These high $\delta^{15}N$-(N_2) values appear to be at least partly, coupled to high $^3He/^4He$ signatures. This suggests that the part of the African Superplume which supplies the northern section of EARS volatile elements, has carbon isotope values identical to those characteristics for the depleted MORB mantle, whereas its nitrogen isotopic values are largely more positive than the upper mantle, suggesting large-scale delivery of modified (mostly likely) recycled nitrogen via the African Superplume. To what degree this applies to other sections of the EARS remains to be tested.

REFERENCES

Barry, P. H., D. R. Hilton, T. P. Fischer, J. M. de Moor, F. Mangasini, and C. Ramirez: Helium and carbon isotope systematics of cold "mazuku" CO2 vents and hydrothermal gases and fluids from Rungwe Volcanic Province, southern Tanzania, *Chem. Geol.*, **339**, (2013), 141–156.

Barry P.H., and Hilton, D.R.: Release of subducted sedimentary nitrogen throughout Earth's mantle. *Geochemical Perspectives Letters*, **2**, (2016) 138-147. doi: 10.7185/geochemlet.1614.

Castillo, PR, DR. Hilton and SA Halldórsson: Trace element and Sr-Nd-Pb isotope geochemistry of Rungwe Volcanic Province, Tanzania: implications for a Superplume source for East Africa Rift magmatism. *Front. Earth Sci*. **2**, (2014), 21. doi: 10.3389/feart.2014.00021.

Cartigny P., Palot M., Thomassot E., Harris J.W.: Diamond formation: A stable isotope perspective. *Annual Review of the Earth and Planetary Sciences* **42**, (2014) 699-732.

Cartigny P., Marty B.: Nitrogen isotopes and mantle geodynamics: The emergence of life and the atmosphere-crust-mantle connection. *Elements* **9**, (2013), 356-366

Craig H. and Lupton, J.E.: Isotope geochemistry and hydrology of geothermal waters in the Ethiopian Rift Valley. *Scripps Inst. Oceanography Technical Rpt*. **77-14**, (1977) p140.

Darrah TH, D.Tedesco, F. Tassi, O.Vaselli, R.J. Poreda: Gas chemistry of the Dallol Geothermal Field of the Danakil Depression in the Afar region of the northern most East African Rift. *Chemical Geology* **339**, (2013), 16-29.

Giggenbach, W.F., Y. Sano, H. Wakita: Isotopes of He, and CO_2 and CH_4 contents in gases produced along the New Zealand part of a convergent plate boundary. *Geochimica et Cosmochimica Acta*, **57** (1993), 3427-3455,

Halldórsson, S.A., D.R. Hilton, V.R. Troll and T.P. Fischer: Resolving volatile sources along the western Sunda arc, Indonesia. *Chemical Geology*, **339**, (2013), 263-282.

Halldórsson, S.A., D.R. Hilton, P. Scarsi, T. Abebe and J. Hopp: A common mantle plume source beneath the entire East African Rift System revealed by coupled helium-neon isotope systematics. *Geophysical Research Letters.* **47**, (2014), doi.org/10.1002/2014GL059424.

Harðardóttir, S., S.A. Halldórsson and D.R. Hilton: Spatial distribution of helium isotopes in Icelandic geothermal fluids and volcanic materials with implications for location, upwelling and evolution of the Icelandic mantle plume. *Chemical Geology*. **480**, (2018), 12-27.

Marty B., Pik R., and Gezahegn Y.: Helium isotopic variations in Ethiopian plume lavas - nature of magmatic sources and limit on lower mantle contribution. *Earth Planet. Sci. Lett.* **144**, (1996) 223-237.

Minissale A, Corti G, Tassi F, Darrah T, Vaselli O, Montanari D, Montegrossi G, Yirgu G, Selmo E, Teclu A.: Geothermal potential and origin of natural thermal fluids in the northern Lake Abaya area, Main Ethiopian Rift, East Africa. *J. Volcanol Geoth Res*. **336**, (2017), 1–18.

Rooney, T. O., B. B. Hanan, D. W. Graham, T. Furman, J. Blichert-Toft, and J.-G. Schilling: Upper mantle pollution during Afar plume–continental rift interaction, *J. Petrol.*, **53**, (2012), 365–389.

Scarsi P. and Craig H.: Helium isotope ratios in Ethiopian Rift basalts. *Earth Planet Sci. Lett.* **144**, (1996) 505-516.

U.S. Environmental Protection Agency, Method 300.0 Determination of inorganic anions by ion chromatography, rev 2.1: Cincinnati, Ohio, Environmental Monitoring and Support Laboratory, (1993), 13 p.